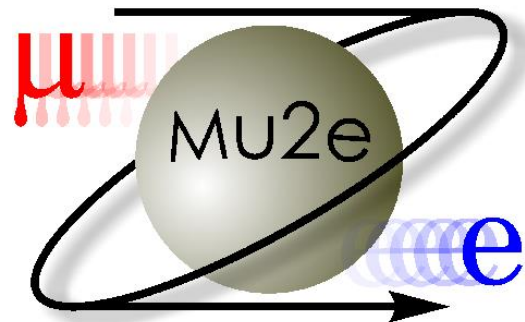


Triangular Counters for Mu2e-II

Ralf Ehrlich
University of Virginia
March 27, 2023



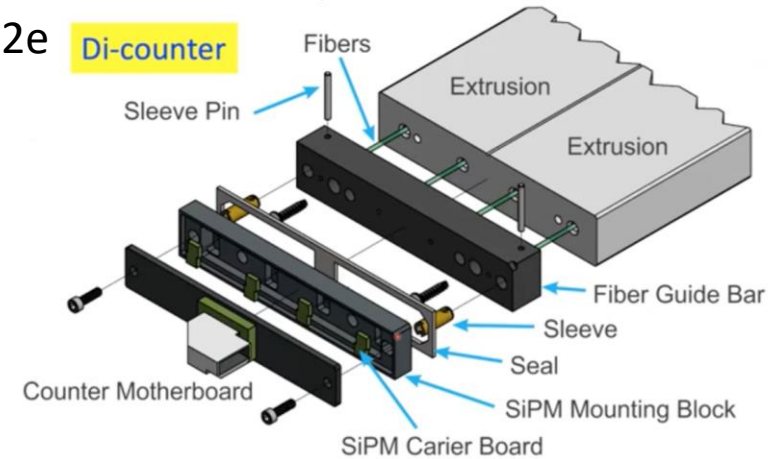
Mu2e-doc-45004-v3



Triangular Counters

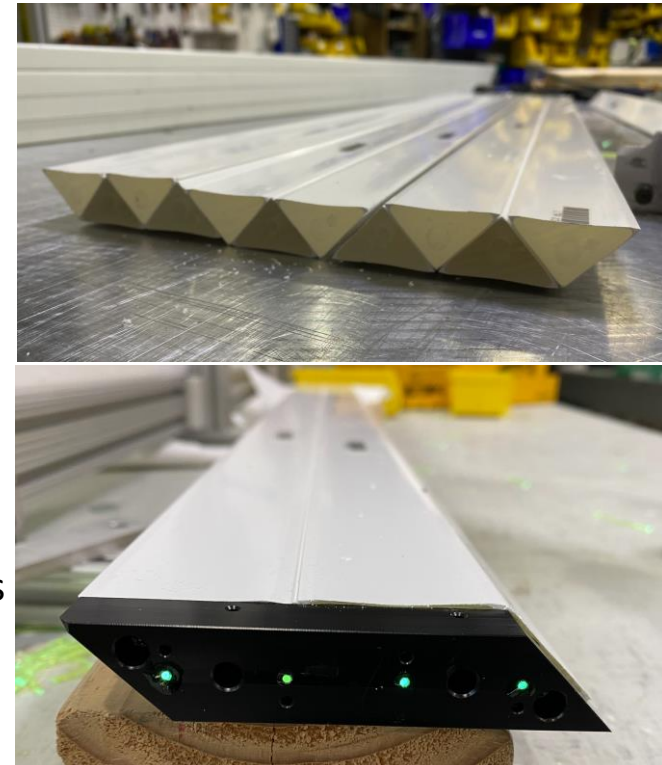
➤ Rectangular counters currently used for the CRV of Mu2e

- Rectangular cross section: 5cm wide, 2cm thick.
- Two fibers per counter.
- One discounter combines two single counters
 - Four channels per “unit”.



➤ New triangular counters proposed for the CRV of Mu2e-II

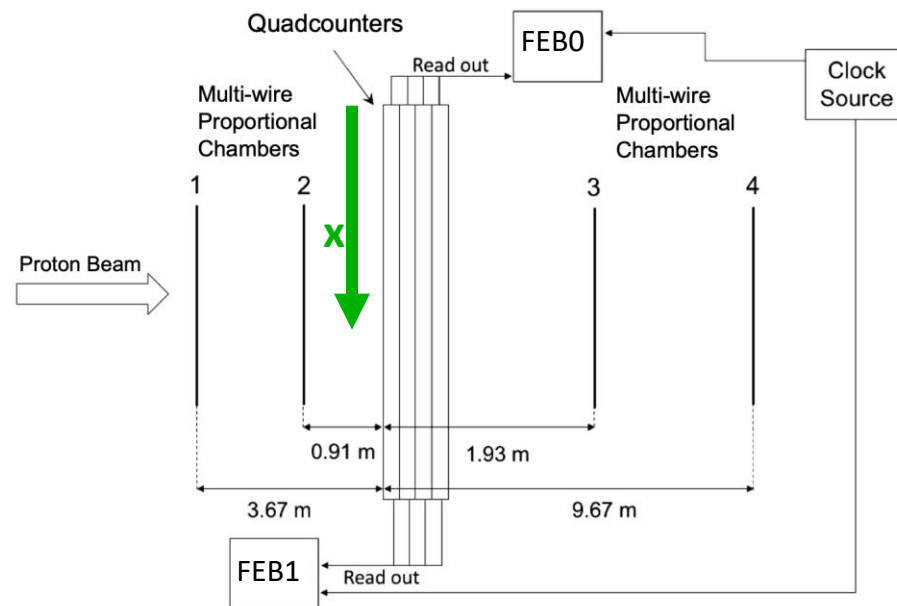
- Triangular cross section: 4cm base, 2cm height.
- One fiber per counter.
- One quadbar combines four single counters
 - Four channels per “unit”.
 - Much of the design of the dicounter electronics can be reused (with adjustments for the different shape).
- These quadbars will allow us to better pin-point the location where tracks went through the counters (using ratios of PEs between adjacent counters).
- Depending on the offset between individual layers, CRV modules made of quadbars may increase the detection efficiency.
 - Simulations need to be done to verify this hypothesis.



Testbeam Setup

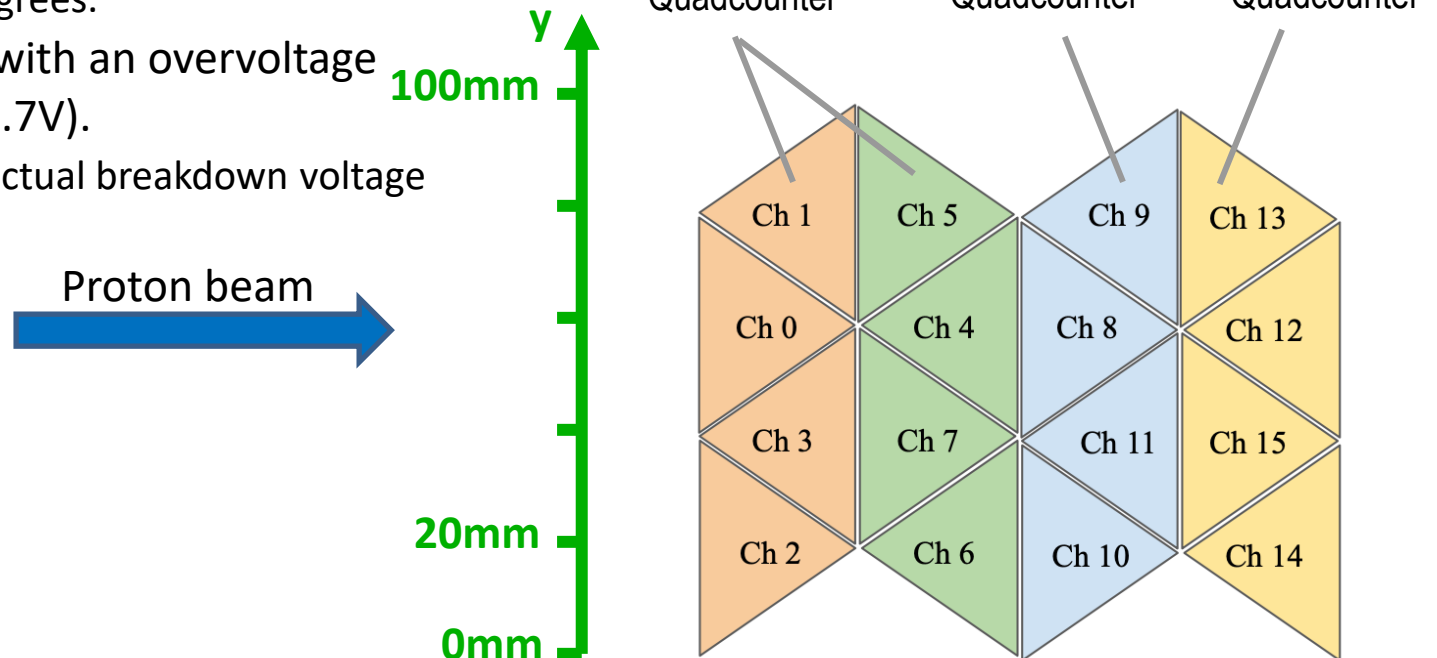
➤ In April 2022, we tested 4 prototype quadbars at Fermilab's testbeam facility.

- Beam: 120 GeV proton.
- Only the two upstream wire chambers worked.
- The FEBs that were used are prototypes of our current FEBs.



Testbeam Setup – Quadbars

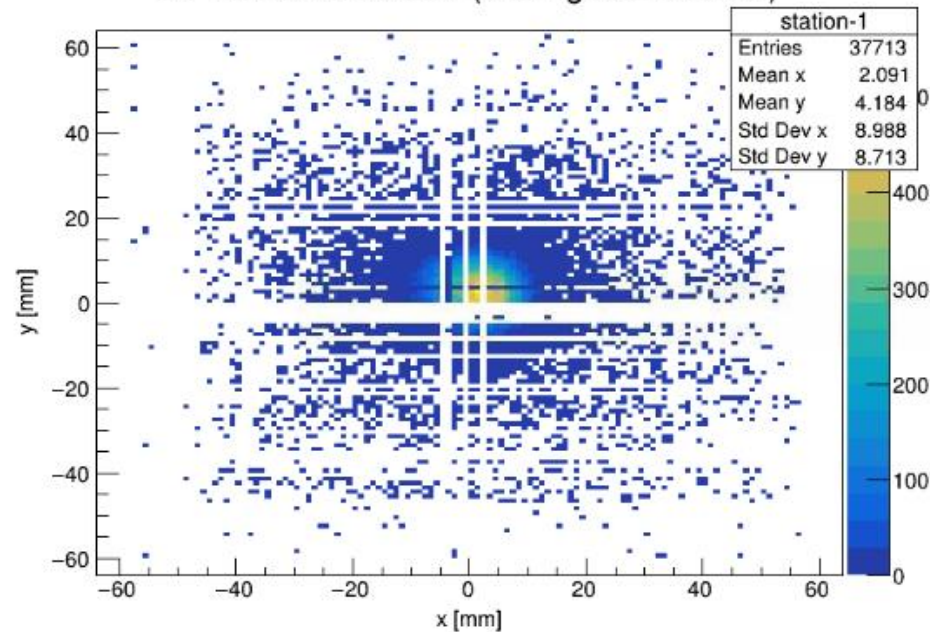
- In April 2022, we tested 4 prototype quadbars at Fermilab's testbeam facility.
 - 2 Quadbars, 3.35m long, unfilled fiber channels
 - 1 Quadbar, 3.35m long, fiber channel filled with Solaris, damaged during production
 - 1 Quadbar, 1m long, unfilled fiber channels
- The proton beam was aimed at
 - x: 80cm from the near readout end (FEB0)
 - y: 24 locations between 15mm and 84mm in steps of 3mm
- Measurements were done with quadbars
 - sitting straight, and
 - tilted by 28 degrees.
- SiPMs were run with an overvoltage of 2.5V (bias ~53.7V).
 - based on the actual breakdown voltage of each SiPM.



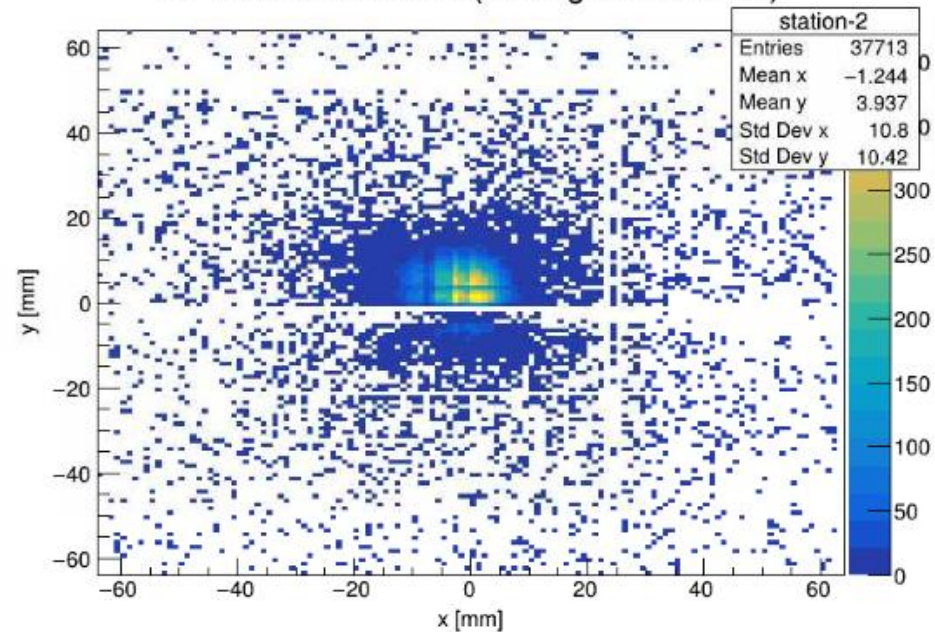
Testbeam Setup – Wire Chambers

- Only two of the four wire chambers were operational.
 - A large fraction of the wires of the operational wire chambers were not working (see plots below).
- Reconstruction efficiency was at 40%, determined by the fraction of events that
 - had at least one hit in each x and y plane of the two wire chambers, and
 - did not have more than two neighboring wires with hits after applying time cuts.

XY Position Station 1 (looking downstream)

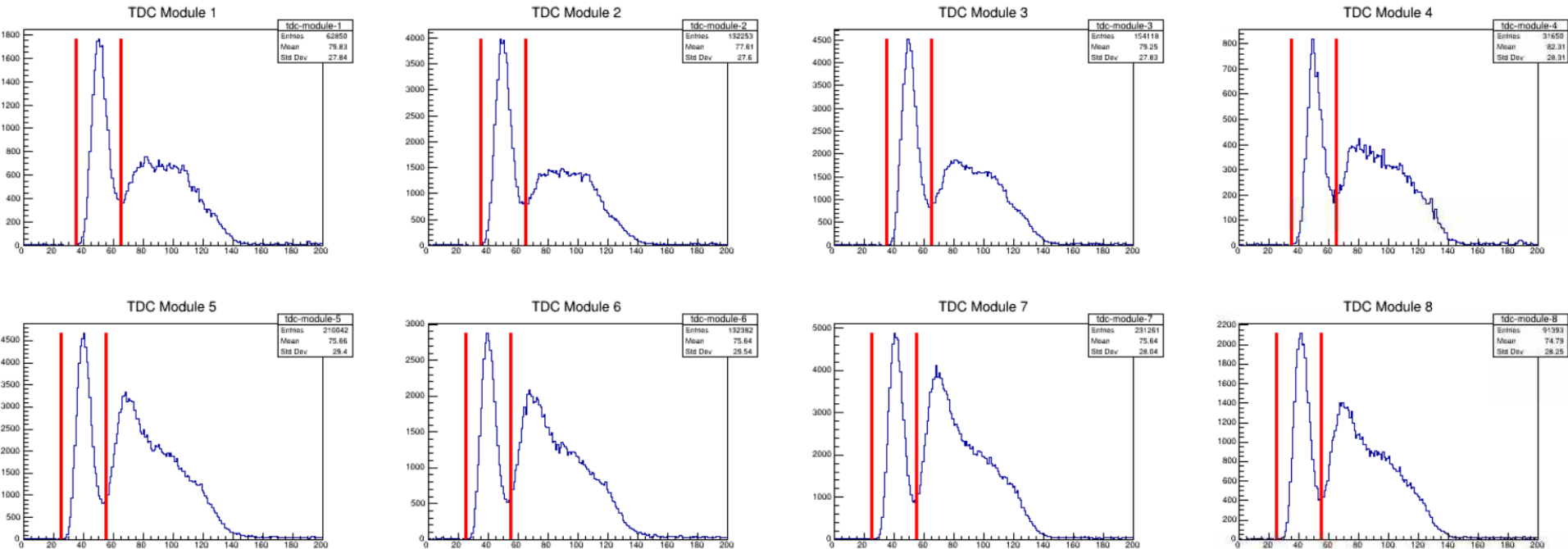


XY Position Station 2 (looking downstream)



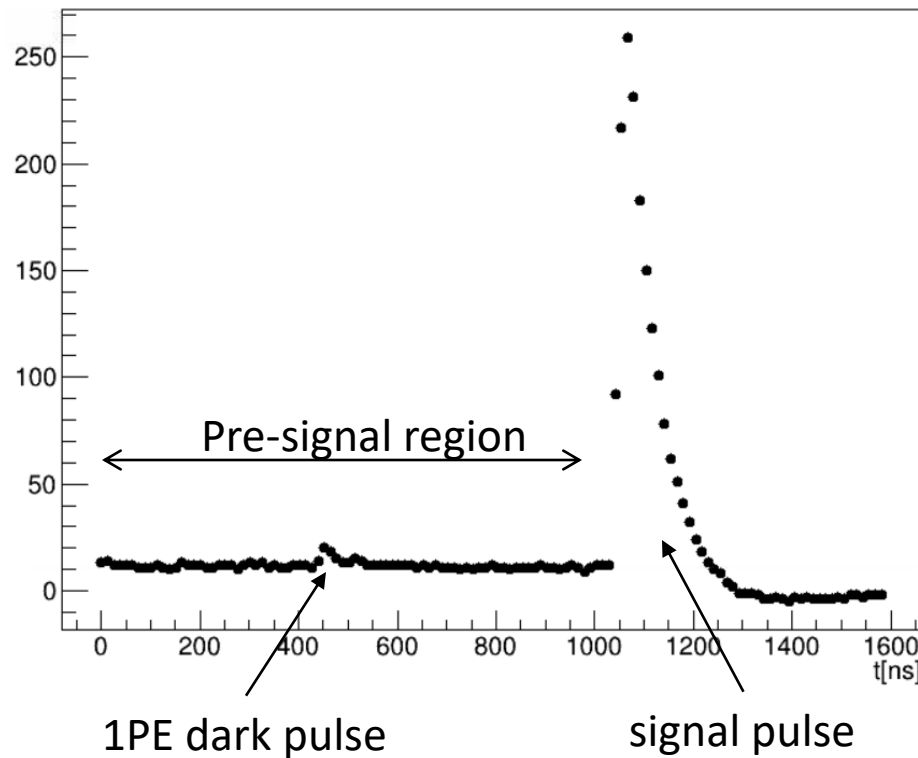
Testbeam Setup – Wire Chambers

- Time cuts applied to the 2 operational wire chambers



Quadbar waveforms

- At every event, we record 127 ADC samples of each channel with 1 ADC sample every 12.5ns.
- The pipeline delay is set to a value which moves the signal peak to $\sim 1100\text{ns}$.
- The pre-signal region ($\sim 1000\text{ns}$ before the signal peak) is used to collect dark noise pulse that are used for the calibration.



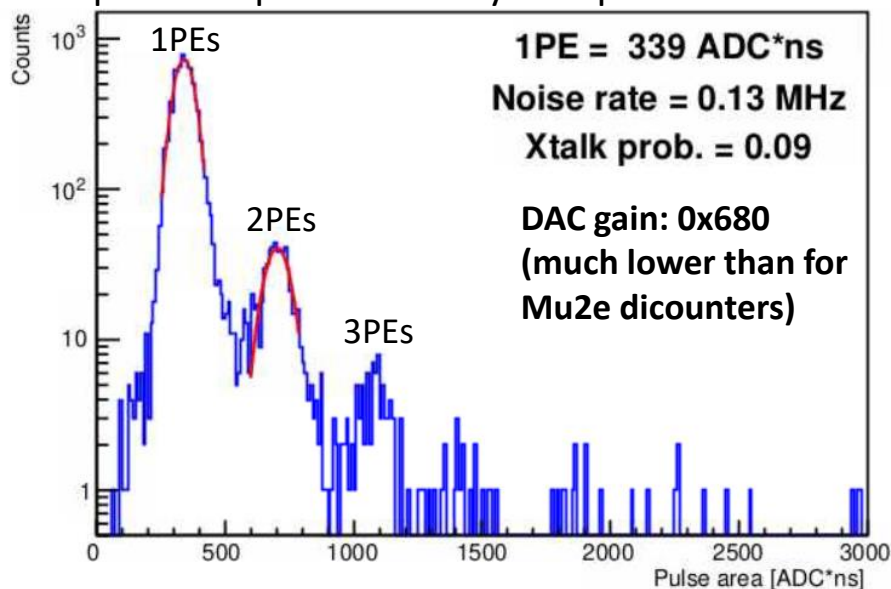
Calibration

- For each channel, the dark pulses from the pre-signal region are collected, reconstructed, and the (pedestal-subtracted) pulse areas are histogrammed.
 - The peaks in the pulse area distribution correspond to 1PE, 2PE, ... dark pulses.
 - These peaks are used to determine the calibration constant, that translates the pulse area into a number of PEs.

Mu2e-II quadbars

Need to fix this problem

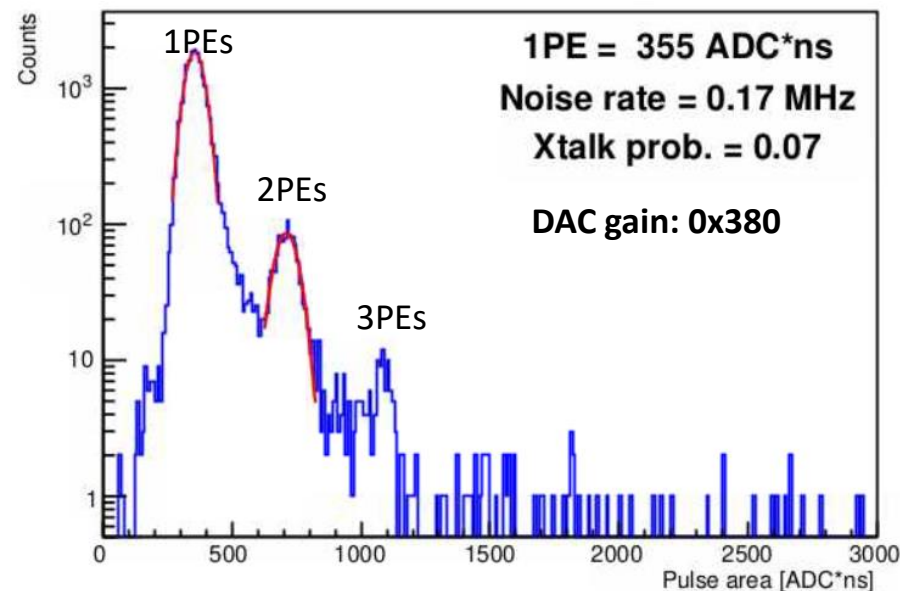
The PE peaks are not precise multiples of each other. Therefore, only the 1PE peak was used. Possible explanation: The fit function that was used may not have been the best choice to describe the pulse shapes created by the quadbar electronics.



Mu2e dicounters

The PE peaks are multiples of each other.

Are we going to use Mu2e or Mu2e-II CMB electronics?



Reconstruction

➤ Pulses are fitted with a modified form of the Gumbel distribution

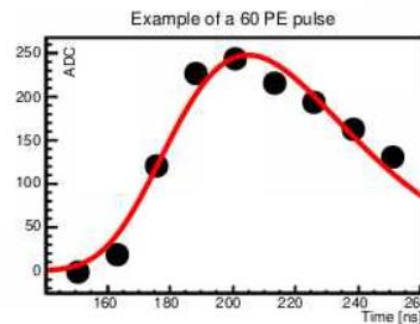
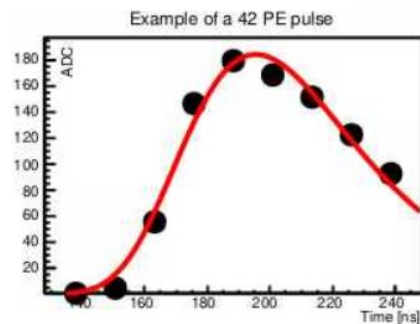
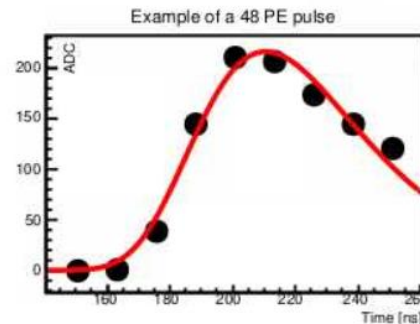
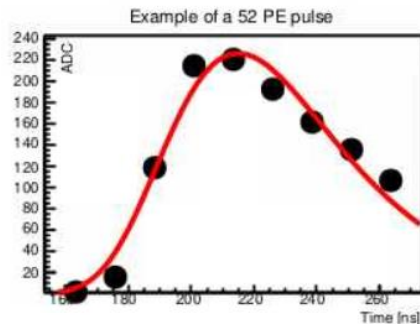
$$ADC(t) = A \cdot e^{-\frac{t-\mu}{\beta}} e^{-\frac{t-\mu}{\beta}}$$

- Pulse height: $\frac{A}{e}$
 - Peak time: μ
 - Pulse area: $A \cdot \beta$
- After the calibration, the pulse areas can get translated into a number of PEs.

← Need to do a chi2 comparison →

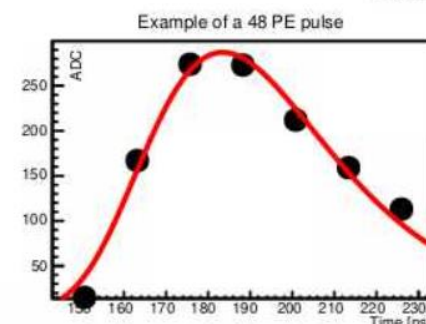
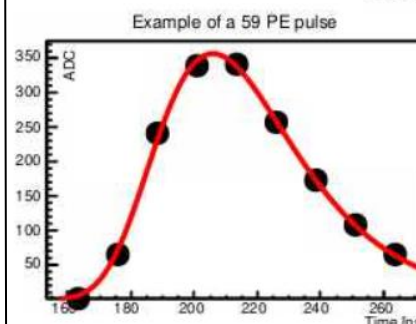
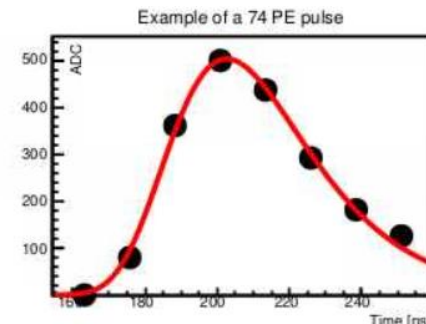
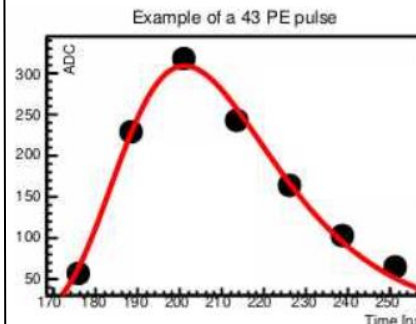
Mu2e-II quadbars

The fit function doesn't seem to do such a good job describing the quadcounter pulses.



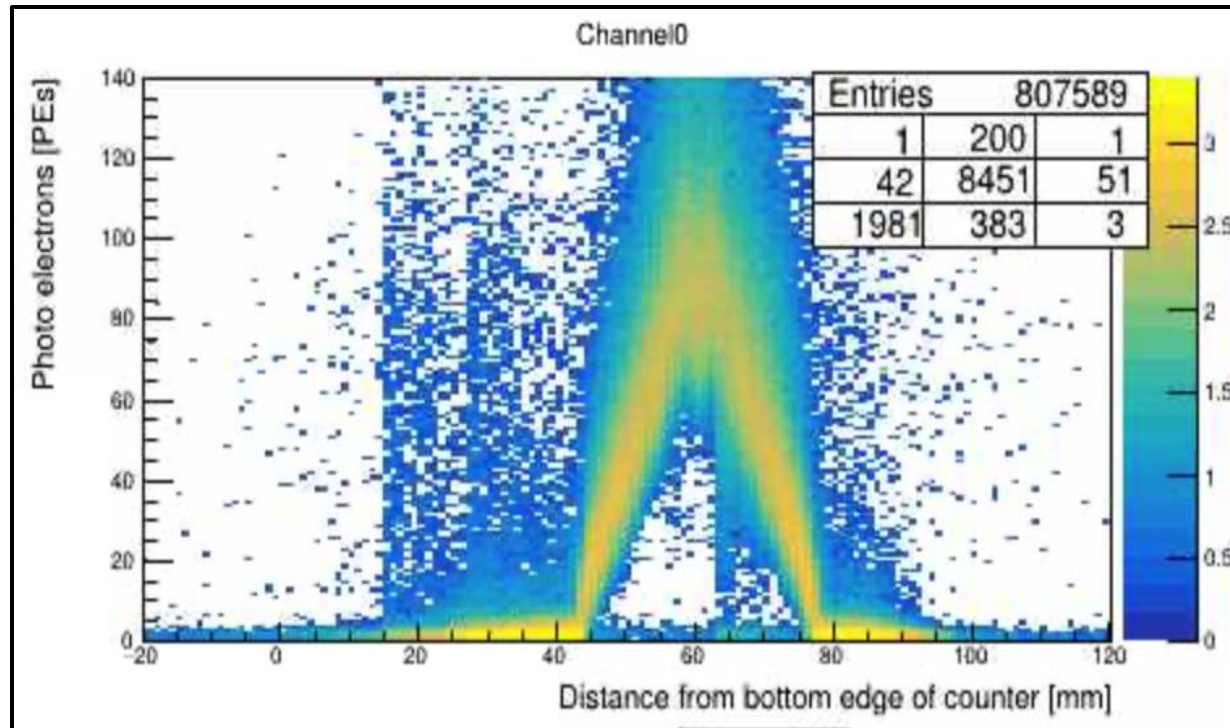
Mu2e dicounters

Pulses from Mu2e dicounters seem to be described well by the fit function.



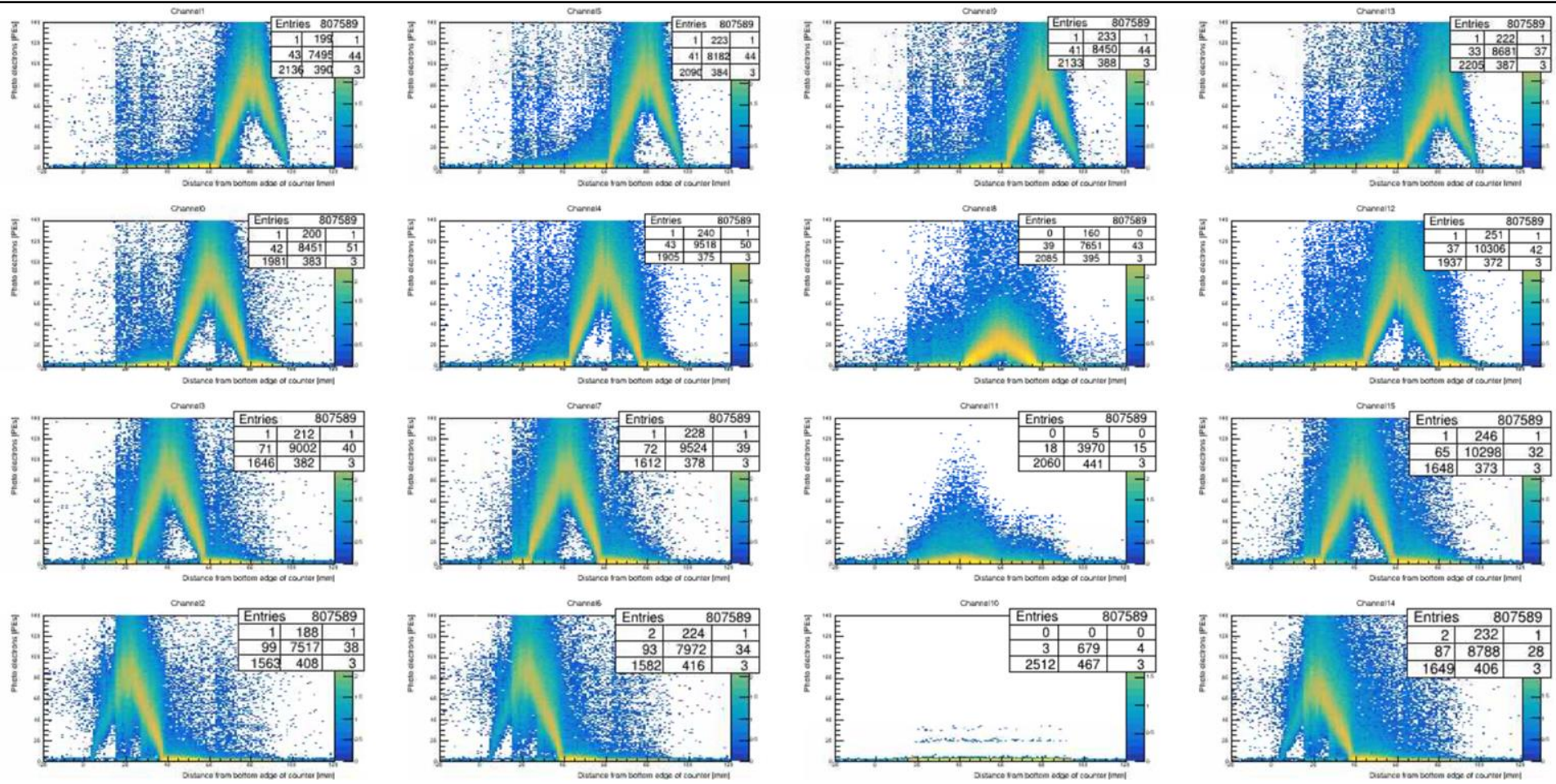
PE yields – One quadbar channel

- PE distribution vs track location at the quadbar (determined by wire chamber).
- This distribution was created combining data of runs across the entire quadbar.
- The triangle shape of the quadbar results in different path length, which leads to the triangle shape of the PE distribution.
- The fiber hole at the center of the triangle creates the small dip at the peak.



PE yields – All quadbar channels

➤ PE distribution vs track location at the quadbar (determined by wire chamber).



Unfilled 3.35 m
Quadcounter

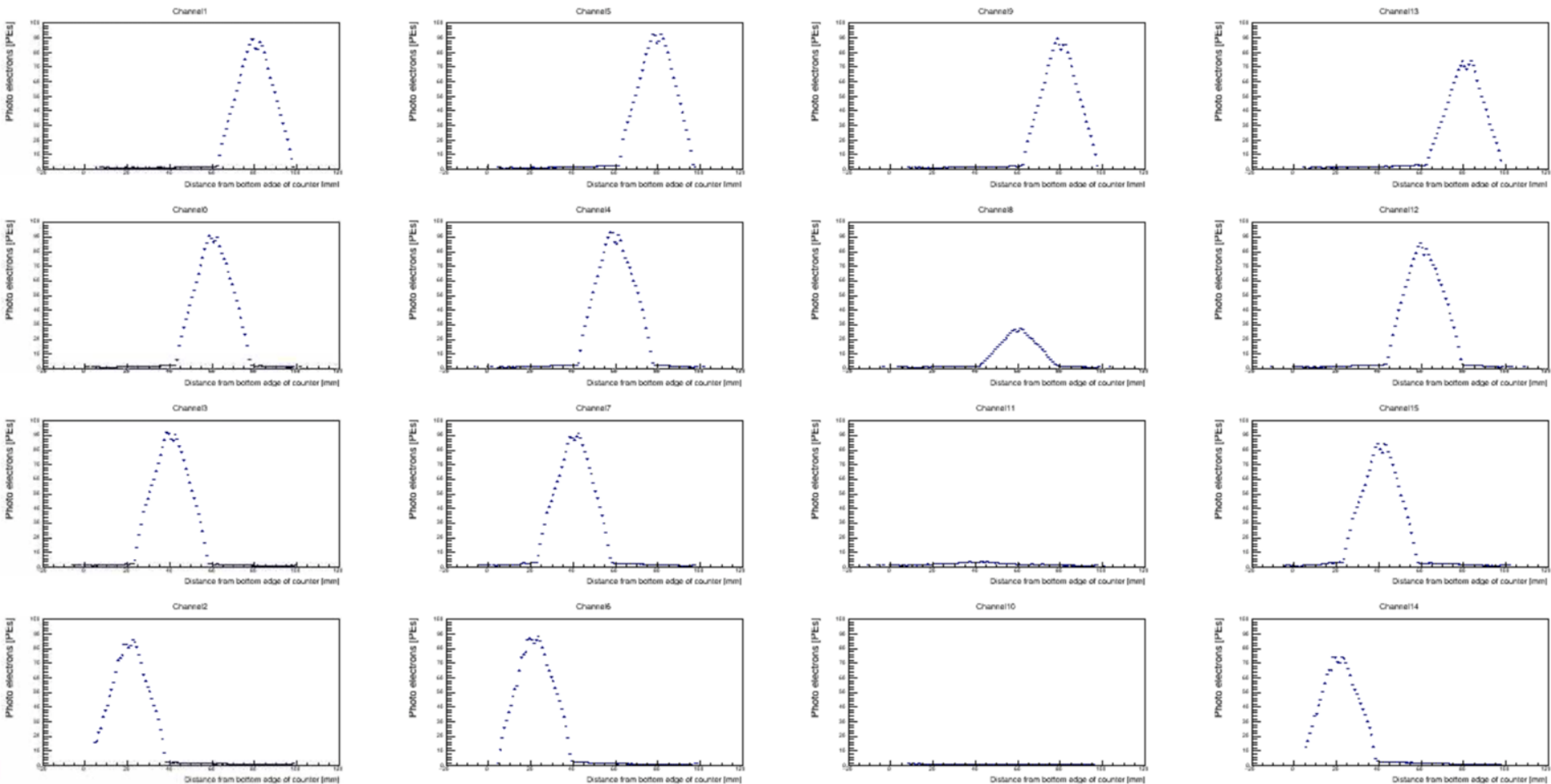
Unfilled 3.35 m
Quadcounter

Damaged Filled 3.35 m
Quadcounter

Unfilled 1 m
Quadcounter

PE yields – All quadbar channels

- Mean PE distribution vs track location at the quadbar (determined by wire chamber).



Unfilled 3.35 m
Quadcounter

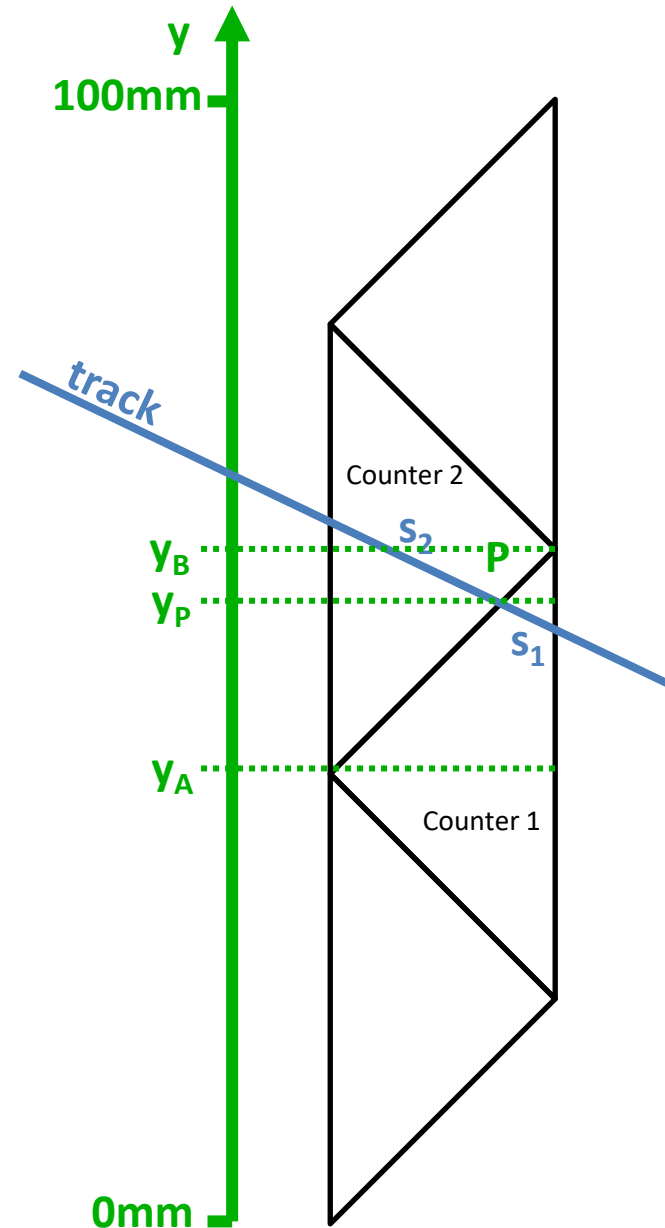
Unfilled 3.35 m
Quadcounter

Damaged Filled 3.35 m
Quadcounter

Unfilled 1 m
Quadcounter

Track positions

- We want to determine the location y_P where the track went through the quadbar using the PE yields of the quadbar.
- The ratio of the PE distributions in counters 1 and 2 is equal to the ratio between the muon path lengths s_1 and s_2 : $\frac{PE_1}{PE_2} = \frac{s_1}{s_2}$
- We also know that $\frac{s_1}{s_2} = \frac{y_B - y_P}{y_P - y_A}$.
- Therefore, we get $y_P = \frac{PE_1 \cdot y_A + PE_2 \cdot y_B}{PE_1 + PE_2}$

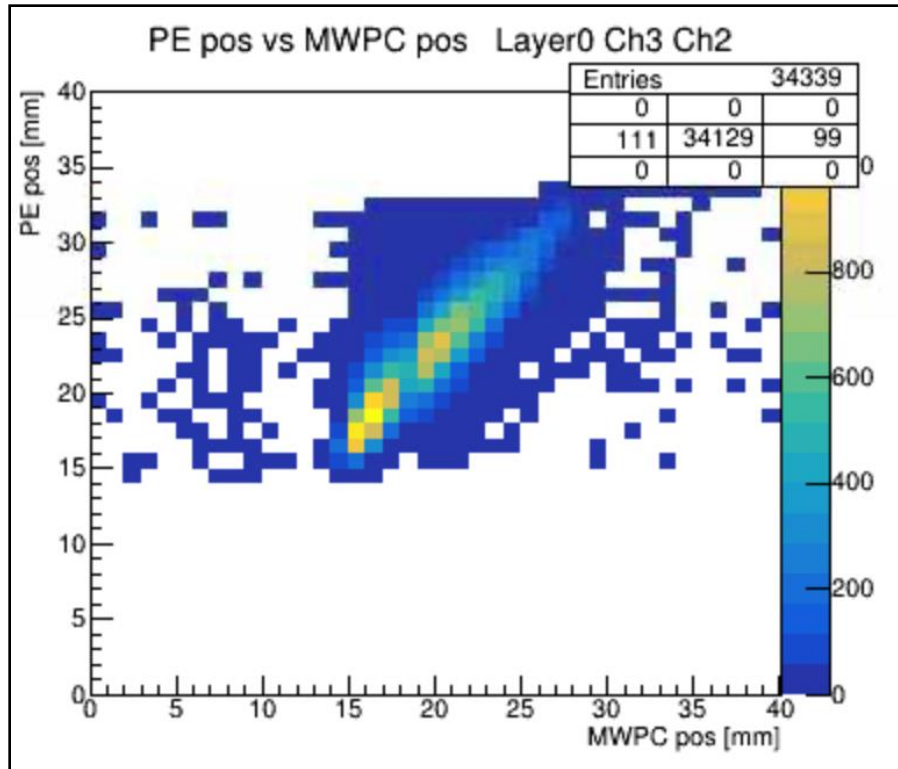


Track position resolution

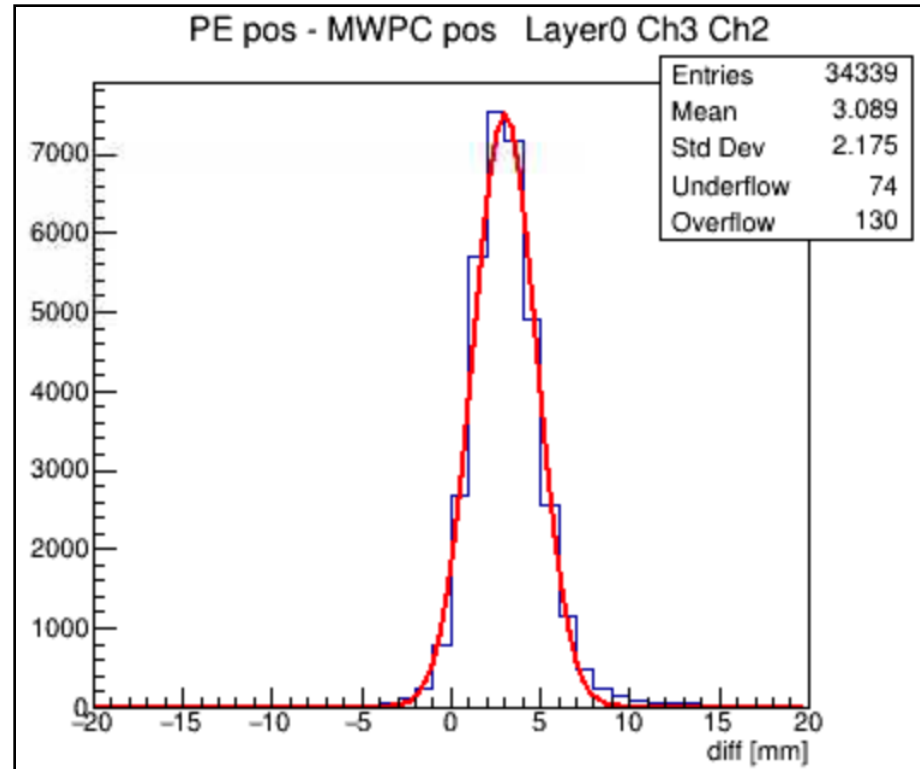
➤ Use only data from individual beam positions (i.e. runs are not combined here)

- Example

Positions determined
by quadcounter vs wirechamber

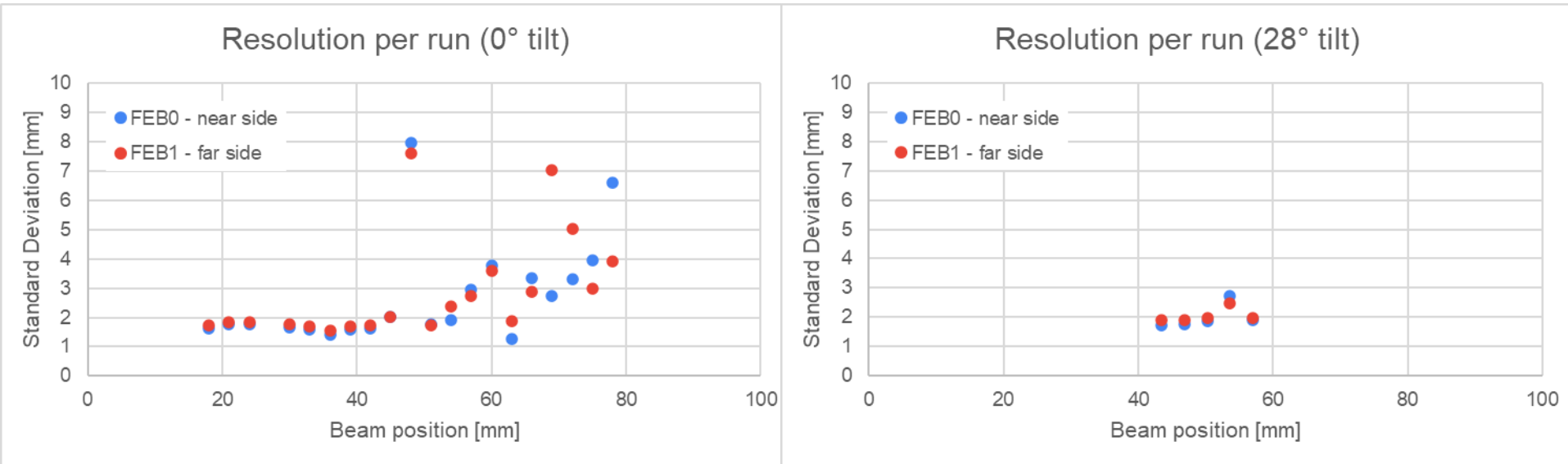


Differences b/w positions determined
by quadcounter and wirechamber



Track position resolution

- Use only data from individual beam positions (i.e. runs are not combined here)



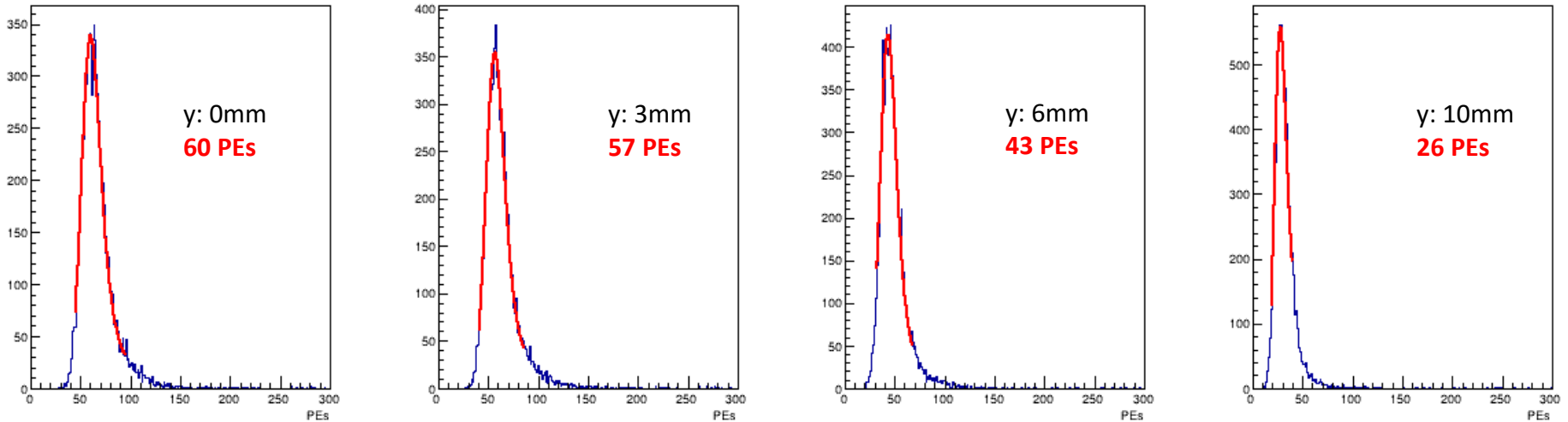
Simulation

- Recently started simulating the response of triangular counters.
- Using updated material constants.
- Testing fiber channels with and without filling (Solaris).
- Testing different coatings.
 - Some of them have a higher reflectivity compared to the currently used TiO_2 coating.
 - Higher reflectivities (e.g. up to 98%) have a significant impact on the light yield due the high number of reflections inside the extrusions.

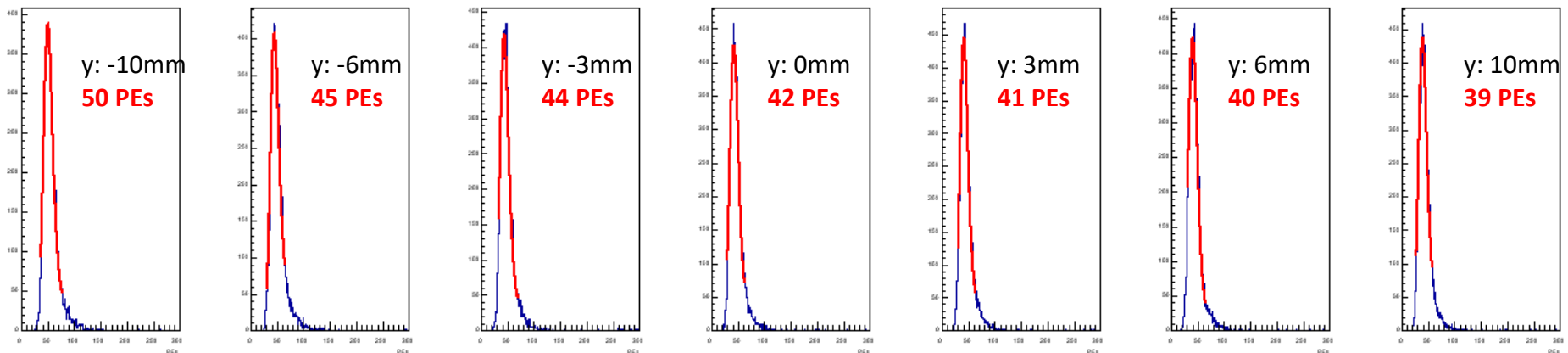
Simulation

➤ Recently started simulating the response of triangular counters.

- Triangular counter, 4cm base, 2cm height, fiber at $y=0\text{mm}$ (center)

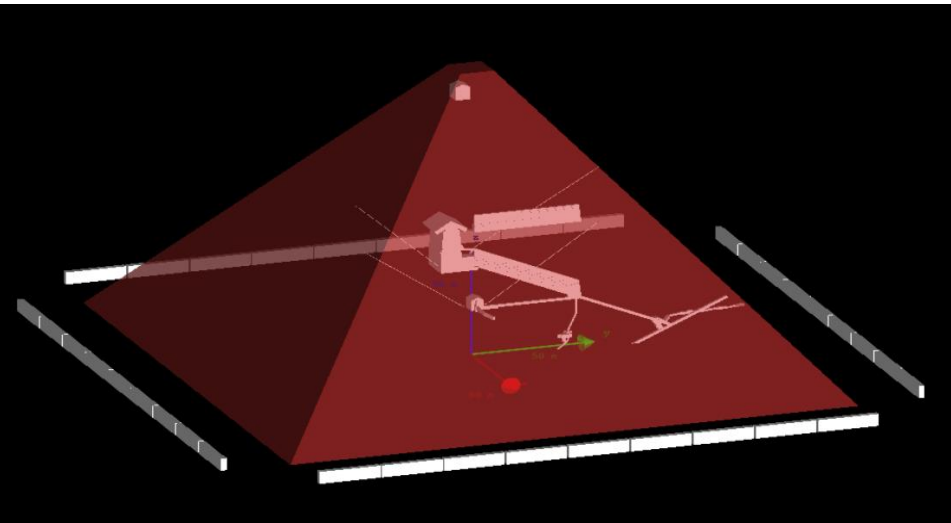


- As a comparison: rectangular counter, 5cm wide, 2cm thick, fibers at $y=-13\text{mm}$ and $+13\text{mm}$, same material properties as triangular counters

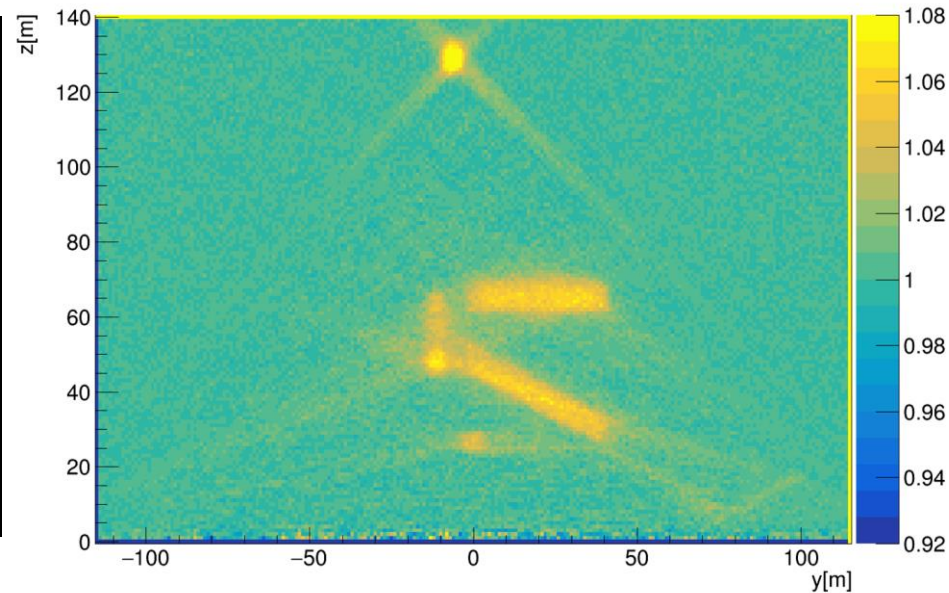


NAUM and EGP projects

- These triangular counters will be used for muography projects to scan the interior of pyramids using cosmic ray muons.
 - The EGP (Exploring the Great Pyramid) project, that will scan the interior of the Great Pyramid in Giza, Egypt.



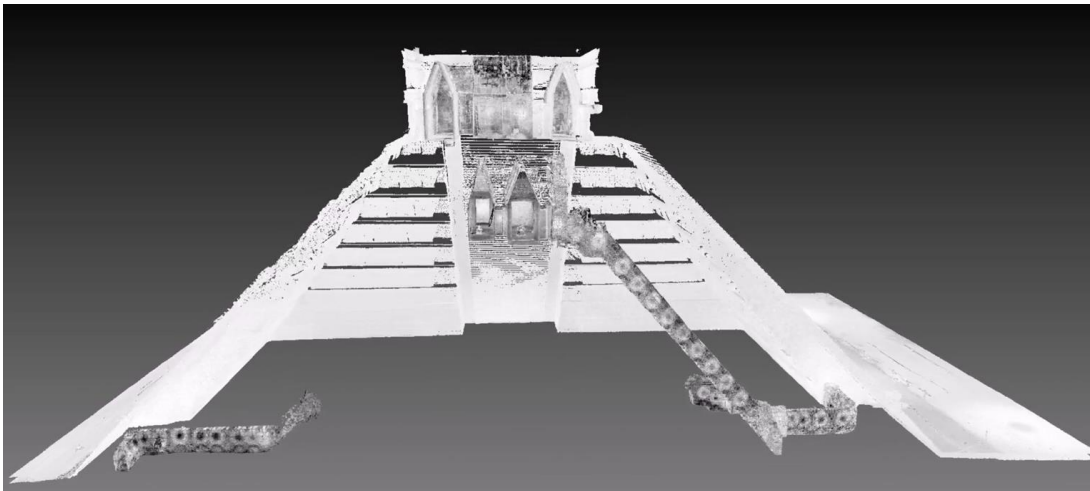
Geant4 model of the pyramid
with two additional hypothetical voids



A slice of the reconstructed 3D image
of the simulated pyramid to the right.

NAUM and EGP projects

- These triangular counters will be used for muography projects to scan the interior of pyramids using cosmic ray muons.
 - The NAUM (Non-invasive Archaeometry Using Muons) project, that will scan the interior of the pyramid at the Maya city Chichén Itzá in Mexico.



Cross section generated from a point cloud flythrough (generated by a Laser scan).